

Detecting oxygen vacancies in SrTiO₃ by 3d transition-metal tracer ions

B. P. Andreasson,* M. Janousch, and U. Staub
Swiss Light Source, Paul Scherrer Institut, 5232 Villigen PSI, Switzerland

T. Todorova and B. Delley
Condensed Matter Theory Group, Paul Scherrer Institut, 5232 Villigen PSI, Switzerland

G. I. Meijer
IBM Research, Zurich Research Laboratory, 8803 Rüschlikon, Switzerland

E. Pomjakushina
Laboratory for Developments and Methods, Paul Scherrer Institut, 5232 Villigen PSI, Switzerland
 (Received 9 November 2009; published 31 December 2009)

X-ray absorption experiments on 3d transition-metal tracer ions in SrTiO₃ are presented. The absorption spectra of the tracer-ion changed upon reduction in the SrTiO₃. This change is due to an oxygen vacancy created at the tracer-ion site. This finding is supported by density-functional theory calculations, which prove that the oxygen vacancies preferentially are created at the tracer-ion sites. Using the chemical sensitivity of x-ray absorption spectroscopy, tracer ions can be used to detect oxygen vacancies in SrTiO₃ and possibly in other oxide systems.

DOI: [10.1103/PhysRevB.80.212103](https://doi.org/10.1103/PhysRevB.80.212103)

PACS number(s): 72.80.Ga, 71.30.+h, 71.55.Ht, 78.70.Dm

3d transition-metal oxides (TMO) present a variety of physical phenomena. The most prominent properties of these oxides are related to their conductivity, e.g., metal-to-insulator transitions,¹ superconductivity,² or colossal magnetoresistance.³ In all these strongly correlated electron systems the stoichiometry as well as the hybridization of the metal 3d electrons with the oxygen ligands are of crucial importance. Consequently, defects, such as oxygen vacancies, strongly influence the properties of TMOs.

Several phenomena have recently been suggested to be directly caused by oxygen vacancies. The resistivity change with applied electric fields seen in some TMOs was proposed to be induced by movements of oxygen vacancies.^{4,5} The metallic interface between the two insulators SrTiO₃ and LaAlO₃ is possibly related to a small number of oxygen vacancies in SrTiO₃, doping it with enough electrons to create metallic conductivity.⁶ Other possibilities for interpretations of the conductivity in this interface are polarity discontinuities⁷ or cationic intermixing.⁸ Also room-temperature ferromagnetic order, which occurs in dilute ferromagnetic oxides, such as Co-doped TiO₂,⁹ has been proposed to occur due to defects close to the surface in the material.¹⁰ Moreover, superconductivity in the iron pnictides has been attributed to oxygen vacancies doping the material.¹¹ All these systems display a variety of physical phenomena where the influence of oxygen vacancies has not yet been elucidated. The presence of less than 4% of oxygen vacancies was up to now difficult to measure experimentally.¹²

The distribution of oxygen vacancies was recently studied in Cr-doped SrTiO₃ crystals by x-ray absorption.^{13–16} It was shown that oxygen vacancies reside preferentially in the first shell of the Cr atom. In this study we clarify the general relation between oxygen vacancies and 3d transition-metal ions inserted in SrTiO₃. We show that these atoms can be used as tracer atoms for oxygen vacancies, i.e., the oxygen

vacancies are preferentially created at the “tracer-ion” sites. This general behavior is further corroborated by density-functional theory (DFT) and multiple-scattering calculations.

Single crystals of SrTiO₃ with 0.2 mol % V, Cr, Mn, Fe, Co, or Ni were grown in a N₂/O₂ atmosphere by floating-zone melting. The precursors were prepared by using a stoichiometric mixture of SrCO₃, TiO₂, and a corresponding tracer-ion oxide. Polycrystalline SrTiO₃ samples with 0.2 mol % Sc, Cu, and Zn were sintered at 1200 °C in air. The group of samples above are called “oxidized” hereafter. A second group was additionally annealed in H₂/Ar (2%/98%) at 1600 °C, hereafter called “reduced.” The oxidized samples were electrically insulating (GΩ cm) and the reduced samples were all electrically conducting (mΩ cm).

X-ray absorption near-edge spectroscopy (XANES) measurements at the *K* edge of the tracer ions were performed at the LUCIA, SuperXAS, and MicroXAS beamlines of the Swiss Light Source at the Paul Scherrer Institut, Switzerland. Data were collected at room temperature in fluorescence yield mode with a silicon-drift detector with an energy resolution of about 150 eV to discriminate the Ti fluorescence. The fluorescent x rays were measured perpendicular to the incoming beam and the sample made an angle of approximately 45° to the incoming beam. To suppress the titanium fluorescence for Cr-Co (Ni-Zn), a 0.5 mm Teflon (0.3 mm aluminum) absorber was used in front of the fluorescence detector.

Figure 1(a) shows the experimental XANES obtained around the tracer-ion *K* edges in SrTiO₃. For each tracer ion, spectra were measured on the oxidized and on the reduced samples. The spectra are vertically stacked for clarity. The energy scale has been shifted with E_0 chosen at half the edge step. Overall, the top eight spectra (Sc to Ni) taken on oxidized samples have similar structures. The weak features prior to the edge are labeled (i), the main edge peak is labeled (ii), and this is followed by another, less pronounced

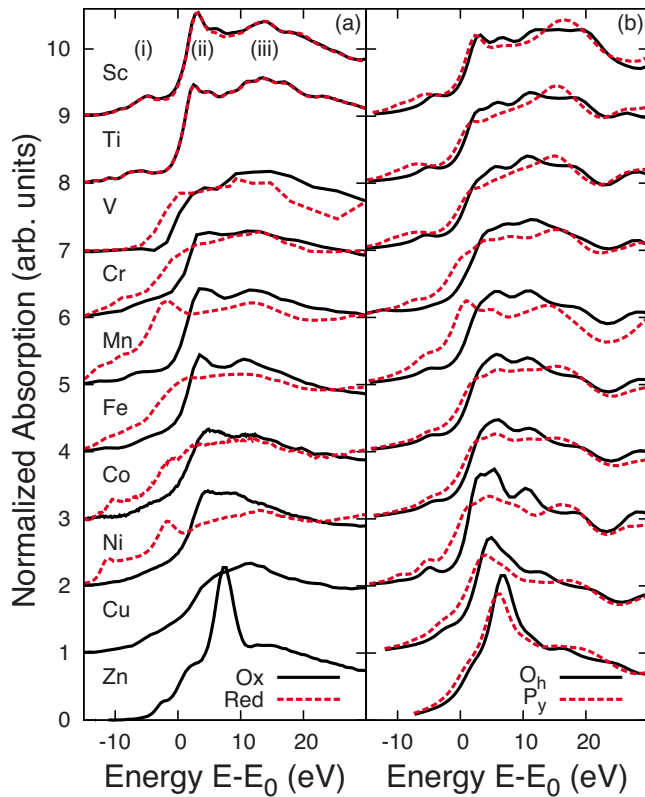


FIG. 1. (Color online) (a) Experimental K -edge XANES spectra measured on the SrTiO_3 samples with different tracer ions (Sc to Zn). Data were taken on oxidized samples (solid lines) and on reduced samples (dashed lines). (b) Multiple-scattering calculations were performed with a full oxygen octahedron surrounding the tracer ion (octahedral coordination, O_h) and with an oxygen vacancy in the first shell surrounding the tracer ion (pyramidal coordination, P_y). The energy scale has been shifted such that the half edge step of the spectra (E_0) measured on oxidized samples (calculated with full octahedron) coincide.

peak, labeled (iii). The Cu spectrum has, contrary to the other spectra, a broader edge structure and the Zn spectrum is dominated by the main edge peak (ii).

Spectra taken on the reduced samples show a general trend with broadened features and a shift of the main edge to lower energies. When measuring the Ti spectra, no difference within the experimental resolution could be detected between the oxidized and the reduced samples. The Ti spectrum in Fig. 1(a) was measured on the sample with Co tracer ions. The Ti spectra of all other samples show the same behavior, indicating that the change leading to electrical conductivity manifests itself only in the spectra from the tracer ions. The spectra acquired on the reduced samples with V to Ni tracer ions exhibit clear shifts toward lower energies and broadening of the spectra. This demonstrates that the electronic states of the tracer ions is strongly affected by oxygen vacancies. After reducing the Cu and Zn samples, the Cu and Zn signals were no longer homogeneously distributed throughout the samples. This indicated that the Cu and Zn ions cluster, thus no longer reflect a homogenous solid solution. Therefore these data were not included in Fig. 1(a).

DFT ground-state calculations¹⁷ of tracer ions in SrTiO_3

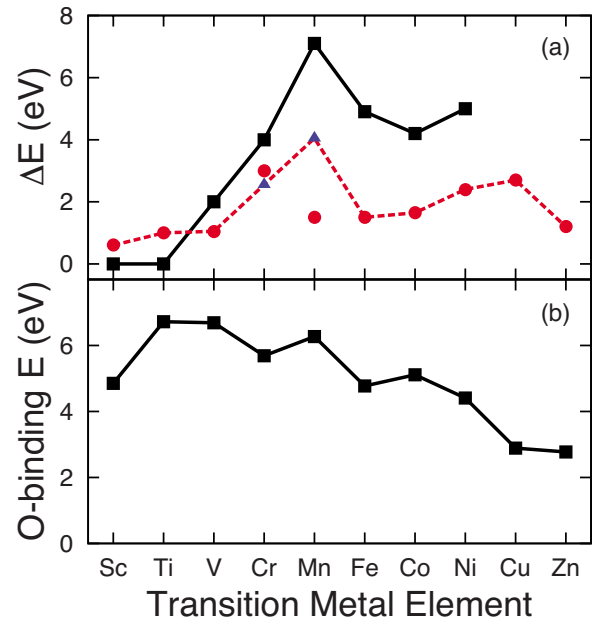


FIG. 2. (Color online) (a) Experimental edge shift of the x-ray absorption spectra due to reduction (solid line) and edge shift for the calculated x-ray absorption spectra induced by introduction of an oxygen vacancy in the first shell of the respective transition-metal element (dashed line). The two triangles depict the edge shift of the calculated Cr and Mn spectra after alteration of the nearest-neighbor distances. (b) Required energy to create an oxygen vacancy in the first shell of the tracer ion obtained by DFT calculations.

were performed. In the computations, supercells of $3 \times 3 \times 3$ unit cells of SrTiO_3 were used where the central Ti atom was replaced by the other $3d$ transition-metal tracer ion. Additional calculations were made with an oxygen vacancy in the nearest-neighbor shell of the tracer ion. In each case, the structure was relaxed to find the energetic minima resulting in the local distortion around the tracer ions. Additionally, these calculations yielded the energy needed to incorporate the tracer ions without, and with an oxygen vacancy in the first shell, resulting in the O-binding energy. Figure 1(b) shows *ab initio* self-consistent real-space multiple-scattering calculations [FEFF 8.4 (Ref. 18)] of the K -edge XANES. They were performed for each incorporated tracer ion using the local structure obtained from the relaxed DFT calculations. For each tracer ion two spectra are presented, one with complete oxygen octahedron and one with an oxygen missing in the first shell surrounding the tracer ion. The calculated spectra for each tracer ion reproduce the measured spectra well. In general, when an oxygen vacancy is introduced, the features are broadened and the edge shifts toward lower energy. This confirms the assumption that the $3d$ tracer ions are incorporated at the Ti site.¹⁹

Figure 2(a) shows the experimental and the calculated energy shift of the absorption edge for each of the tracer ions in reduced SrTiO_3 samples. This shift (ΔE) is the difference of the energy values (E_0) between the spectra obtained from reduced and oxidized samples. The experimental shifts (squares) show an increasing trend throughout the $3d$ series with a clear maximum for Mn. The same trend is found for

the theoretical shifts (circles) but without the pronounced maximum for Mn. The triangles depict two additional calculations performed with altered atom positions. These clearly increase the similarities between theory and experiment, cf., solid and dashed line, discussed in detail below.

The exaggerated hybridization in the usual approximations of DFT leads to an underestimation of the edge shift on reducing the samples, as seen in Fig. 2(a). In the case of Mn the crossover from the trend of light transition metals to the heavy first row transition metals is missed too. If hybridization is broken by using a single-ion model, an overestimated edge shift appears, even if full screening by $4s$ and $4p$ electrons is taken into account. This line of reasoning corroborates the idea that the hybridization acts to reduce the observed edge shift on reduction. However, the hybridized DFT model comes out significantly closer to the observed shift, albeit with an underestimation factor of about 2.

Figure 2(b) shows the calculated energy difference for incorporating the tracer ions at the Ti position with and without oxygen vacancy in the surrounding first shell. The energy for creating an oxygen vacancy on Ti is largest and the lowest energy is found for Zn. This proves that oxygen vacancies are preferentially created at tracer-ion sites. [Note: The O-binding energies in Fig. 2(b) do not reflect how much energy is required to incorporate the tracer ions.²⁰]

The position of the edge in the FEFF-calculated spectra was on average within 3 eV of the experimental edge. When spectra were compared, each calculated spectrum with full octahedron was shifted 2–4 eV to coincide with the experimental spectrum of the oxidized sample. When the atom positions obtained by DFT calculations were used to calculate the Cr and Mn spectra with a vacancy in the first shell, significant discrepancies with the measured spectra were found, cf., reduced and Orig in Figs. 3(a) and 3(b). The nearest-neighbor distance from DFT represents a standard distance for octahedrally coordinated Cr and Mn, corresponding to 2.6+ and 3+, respectively.²¹ Agreement was obtained when the Cr-O distances were decreased by 5% [Mod in Fig. 3(a)] and the Mn-O distances were increased by 10% [Mod in Fig. 3(b)]. The physical interpretation is that in the oxidized sample Cr^{4+} is surrounded by a full oxygen octahedron and in the reduced sample the Cr ion is reduced to Cr^{3+} with an oxygen vacancy in the first shell. For Mn, when compared to an octahedrally coordinated Mn^{3+} reference, the measured Mn spectra appears to have lower valence than the reference (shifted toward lower energies). The modified nearest-neighbor distance increase of 10% corresponds to Mn^{2+} -O distances.²¹ This is in agreement with results of early electron paramagnetic resonance (EPR) experiments in Mn-doped SrTiO_3 when annealed in H_2/N_2 .²² In the samples with Mn tracer ions, Mn is 4+ with a full nearest-neighbor oxygen shell in the oxidized sample and 2+ in the reduced sample with an oxygen vacancy in the first shell.

EPR and Mössbauer experiments are supporting these valence changes with reduction. It was shown that for a small amount (<1%) of $3d$ transition-metal ions in SrTiO_3 , no charge-compensating oxygen vacancies were intrinsically observed and the valence was reported to shift up or down when annealed in reducing or oxidizing atmospheres.^{23,24} Our findings show similar trends as recent EPR results.^{25,26}

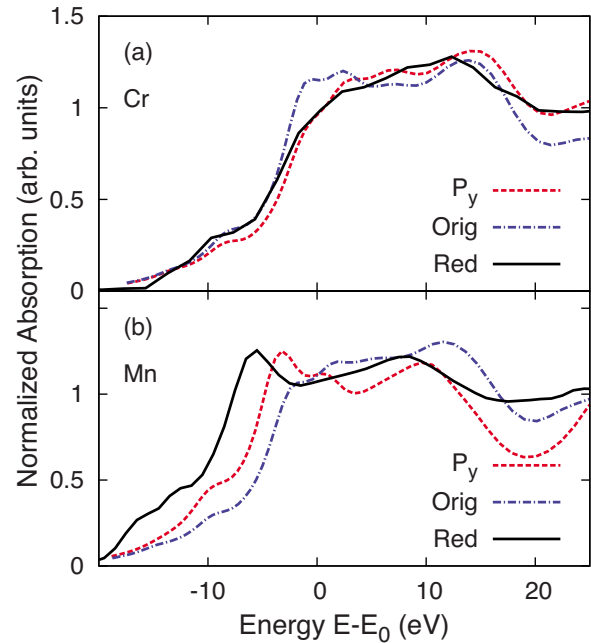


FIG. 3. (Color online) Calculated spectra based on atom positions with an oxygen vacancy in the tracer-ion first shell (pyramidal coordination) compared with spectra measured on the reduced samples for (a) Cr and (b) Mn. In each case, the measured spectrum (solid lines) was compared with the calculation based on the original relaxed atom positions (dash-dot lines) and the calculation based on the atom positions with the altered nearest-neighbor distances (dashed lines).

The fact that all the K -edge data, except for the Ti K edge, show a shape change and particularly an energy shift upon reduction is strong evidence that the main change in the system after reduction takes place in the vicinity of the tracer ions. The spectra calculated with a first shell oxygen agree well with this general trend. It is therefore assumed that when oxygen ions are removed in the reduction process, they are preferably removed from oxygen octahedrons surrounding tracer ions. This is further supported by the O-binding energies calculated with DFT, Fig. 2(b), where Ti has the highest O-binding energy.

From the results presented in Fig. 1(a), a direct quantification of the oxygen vacancy concentration in the reduced samples is not possible. We assume that spectra labeled “Red” in Fig. 1(a) represent cases where all the tracer ions have an oxygen vacancy in the first shell. These spectra therefore correspond to an actual oxygen vacancy concentration of larger than 1/3 of 0.2% or 6.7×10^{-4} . It is larger because it is likely that additional oxygen vacancies are introduced at Ti sites due to the high-temperature reduction. Vacancies further away than the first oxygen shell around a tracer ion are more difficult to detect with x-ray absorption, as the spectral changes are smaller. It is particularly difficult when there is already a vacancy in the first shell, unless there is a clear reference system with a single vacancy to compare the spectral shape with. Therefore, an accurate determination is only valid for concentrations of vacancies lower than the tracer-ion concentration.

The localization of oxygen vacancies by tracer ions in

SrTiO₃ might be a more general trend in TMOs. Intuitively, one may argue that oxygen can be removed more easily at positions where perfect order is disturbed by any kind. Therefore, to probe for vacancies in a TMO, small amounts of tracer ions could be introduced which then may act as vacancy getters. Due to its chemical sensitivity, x-ray absorption spectroscopy at the relevant energy of the tracer ion can give information on the distribution and the concentration of vacancies. In principle, when the tracer-ion concentration is larger than the oxygen vacancy concentration, then a quantitative estimate of the vacancy concentration can be obtained by a fit of the observed spectra to a linear combination of the spectra with and without vacancy. However, this will only be meaningful, if in the studied system, these vacancies at the tracer ion are responsible for the electronic properties of the material, e.g., the conductance. Otherwise, one cannot conclude that the vacancies are responsible for conduction nor can its concentration be quantified in the undisturbed system. On the other hand, the absence of vacancies prove, that conductivity is not related to vacancies and if one observes vacancies, it is still a clear indication of a past presence of a reducing atmosphere, supporting an oxygen vacancies scenario for the origin of electrical conductance. It would be

very interesting to test these expectations by further x-ray absorption spectroscopy studies on other systems.

In conclusion, we presented x-ray absorption data on the 3*d* transition-metal *K* edges of tracer ions in as grown and reduced SrTiO₃. Spectral changes occur systematically on the tracer-ion data but not on the Ti XANES, which indicates the creation of oxygen vacancies at the tracer-ion sites upon reduction. This finding is supported by density-functional theory calculations, which prove that the oxygen vacancies preferentially are created at the tracer-ions sites. Using the chemical sensitivity of x-ray absorption spectroscopy, tracer ions can be used to detect oxygen vacancies and are an indicator of the presence of previous reducing atmospheres in SrTiO₃. These results can likely be applied to other oxide systems, where the role of oxygen vacancies for the electrical properties are unclear.

We thank C. Borca, D. Grollmund, M. Harfouche, and M. Nachtgeaal for support during the beamtimes, S. F. Karg, J. G. Bednorz, and R. Allenspach for discussions, and R. Wetter for technical support. This work was partly supported by the NCCR MaNEP project and performed at the Swiss Light Source, Paul Scherrer Institut, Villigen, Switzerland.

*pererik.andreasson@psi.ch

- ¹M. Imada, A. Fujimori, and Y. Tokura, *Rev. Mod. Phys.* **70**, 1039 (1998).
- ²J. G. Bednorz and K. A. Müller, *Z. Phys. B: Condens. Matter* **64**, 189 (1986).
- ³R. von Helmolt, J. Wecker, B. Holzapfel, L. Schultz, and K. Samwer, *Phys. Rev. Lett.* **71**, 2331 (1993).
- ⁴R. Waser and M. Aono, *Nature Mater.* **6**, 833 (2007).
- ⁵K. Szot, W. Speier, G. Bihlmayer, and R. Waser, *Nature Mater.* **5**, 312 (2006).
- ⁶G. Herranz, M. Basletić, M. Bibes, C. Carrétéro, E. Tafrá, E. Jacquet, K. Bouzouane, C. Deranlot, A. Hamzić, J.-M. Broto *et al.*, *Phys. Rev. Lett.* **98**, 216803 (2007).
- ⁷A. Ohtomo and H. Y. Hwang, *Nature (London)* **427**, 423 (2004).
- ⁸P. R. Willmott, S. A. Pauli, R. Herger, C. M. Schlepütz, D. Marzocchia, B. D. Patterson, B. Delley, R. Clarke, D. Kumah, C. Cionca *et al.*, *Phys. Rev. Lett.* **99**, 155502 (2007).
- ⁹Y. Matsumoto, M. Murakami, T. Shono, T. Hasegawa, T. Fukumura, M. Kawasaki, P. Ahmet, T. Chikyow, S. Koshihara, and H. Koinuma, *Science* **291**, 854 (2001).
- ¹⁰J. M. D. Coey, M. Venkatesan, and C. B. Fitzgerald, *Nature Mater.* **4**, 173 (2005).
- ¹¹J. J. Hamlin, R. E. Baumbach, D. A. Zocco, T. A. Sayles, and M. B. Maple, *J. Phys.: Condens. Matter* **20**, 365220 (2008).
- ¹²D. A. Muller, N. Nakagawa, A. Ohtomo, J. L. Grazul, and H. Y. Hwang, *Nature (London)* **430**, 657 (2004).
- ¹³B. P. Andreasson, M. Janousch, U. Staub, and G. I. Meijer, *Appl. Phys. Lett.* **94**, 013513 (2009).
- ¹⁴M. Janousch, G. I. Meijer, U. Staub, B. Delley, S. F. Karg, and B. P. Andreasson, *Adv. Mater. (Weinheim, Ger.)* **19**, 2232 (2007).
- ¹⁵B. P. Andreasson, M. Janousch, U. Staub, G. I. Meijer, and B. Delley, *Mater. Sci. Eng., B* **144**, 60 (2007).
- ¹⁶G. I. Meijer, U. Staub, M. Janousch, S. L. Johnson, B. Delley, and T. Neisius, *Phys. Rev. B* **72**, 155102 (2005).
- ¹⁷B. Delley, *J. Chem. Phys.* **113**, 7756 (2000).
- ¹⁸A. L. Ankudinov, B. Ravel, J. J. Rehr, and S. D. Conradson, *Phys. Rev. B* **58**, 7565 (1998).
- ¹⁹The Ti spectrum would show the same behavior as the tracer ions if sufficient ($\geq 3\%$) Ti ions had one missing oxygen in their first shell.
- ²⁰The energy cost to incorporate Cu and Zn is approximately 5 eV higher than for the other tracer ions, according to the DFT calculations, indicating that these elements might not prefer to be kept in the SrTiO₃ matrix.
- ²¹N. E. Brese and M. O'Keeffe, *Acta Crystallogr., Sect. B: Struct. Sci.* **47**, 192 (1991).
- ²²K. Blazey, J. Cabrera, and K. Müller, *Solid State Commun.* **45**, 903 (1983).
- ²³E. S. Kirkpatrick, K. A. Müller, and R. S. Rubins, *Phys. Rev.* **135**, A86 (1964).
- ²⁴V. G. Bhide and H. C. Bhasin, *Phys. Rev.* **172**, 290 (1968).
- ²⁵M. E. Zvanut, S. Jeddy, E. Towett, G. M. Janowski, C. Brooks, and D. Schlom, *J. Appl. Phys.* **104**, 064122 (2008).
- ²⁶F. La Mattina, J. G. Bednorz, S. F. Alvarado, A. Shengelaya, and H. Keller, *Appl. Phys. Lett.* **93**, 022102 (2008).